NAVAL POSTGRADUATE SCHOOL

MONTEREY, CALIFORNIA

THESIS

IN-SITU OPTICAL IMAGING OF CARRIER TRANSPORT IN MULTILAYER SOLAR CELLS

by

Brian Craig Rauscher

June 2008

Thesis Advisor:	Nancy Haegel
Second Reader:	Gamani Karunasiri

Approved for public release; distribution is unlimited

THIS PAGE INTENTIONALLY LEFT BLANK

REPORT DOCUMENTATION PAGE		Form Approved OMB No. 0704-0188

1. AGENCY USE ONLY *(Leave blank)*	2. REPORT DATE	3. REPORT TYPE AND DATES COVERED
	June 2008	Master's Thesis

4. TITLE AND SUBTITLE In-Situ Optical Imaging of Carrier Transport in Multilayer Solar Cells	5. FUNDING NUMBERS
6. AUTHOR(S) Brian Craig Rauscher	
7. PERFORMING ORGANIZATION NAME(S) AND ADDRESS(ES) Naval Postgraduate School Monterey, CA 93943-5000	8. PERFORMING ORGANIZATION REPORT NUMBER
9. SPONSORING /MONITORING AGENCY NAME(S) AND ADDRESS(ES) N/A	10. SPONSORING/MONITORING AGENCY REPORT NUMBER

11. SUPPLEMENTARY NOTES The views expressed in this thesis are those of the author and do not reflect the official policy or position of the Department of Defense or the U.S. Government.

12a. DISTRIBUTION / AVAILABILITY STATEMENT	12b. DISTRIBUTION CODE
Approved for public release; distribution is unlimited	

13. ABSTRACT (maximum 200 words)

The goal of this thesis is to explore the utility of in-situ optical imaging of charge transport imaging in multi junction solar cells. An in-situ measurement of a manufactured solar cell's key material parameters is difficult. Many sophisticated models may be used to predict performance of new cell arrangements and suggest next generation improvements. In parallel, an experimental view into a complex, multi layered, alloyed semiconductor device can provide important feedback for material growth and device fabrication.

This body of work builds on the previous work of extracting estimated minority carrier diffusion lengths from multi junction solar cell materials. Indium Gallium Phosphide double heterostructures have been investigated previously with effective results. A technique to estimate electron diffusion length from a luminescent sample intensity distribution has been developed.

This thesis investigates imaging transport and applying the diffusion length estimation directly in the triple junction device. Luminescence from individual layers was isolated using optical filters. The effect of varying temperature and applying bias during the imaging technique is investigated as well. A strong dependence of effective diffusion length on environmental temperature was measured. In addition, a weak dependence of effective diffusion length on bias was measured, with the effect slightly greater in the top, as compared to the central cell.

14. SUBJECT TERMS Solar Cells, Triple Junction Solar Cells, Semiconductor, Diffusion Length	15. NUMBER OF PAGES 59
	16. PRICE CODE

17. SECURITY CLASSIFICATION OF REPORT	18. SECURITY CLASSIFICATION OF THIS PAGE	19. SECURITY CLASSIFICATION OF ABSTRACT	20. LIMITATION OF ABSTRACT
Unclassified	Unclassified	Unclassified	UU

NSN 7540-01-280-5500

Standard Form 298 (Rev. 8-98)
Prescribed by ANSI Std. Z39.18

THIS PAGE INTENTIONALLY LEFT BLANK

Approved for public release; distribution is unlimited

IN-SITU OPTICAL IMAGING OF CARRIER TRANSPORT IN MULTILAYER SOLAR CELLS

Brian Craig Rauscher
Lieutenant, United States Navy Reserve
B.S., Oregon State University, 1997

Submitted in partial fulfillment of the
requirements for the degree of

MASTER OF SCIENCE IN APPLIED PHYSICS

from the

NAVAL POSTGRADUATE SCHOOL
June 2008

Author: Brian Craig Rauscher

Approved by: Nancy M. Haegel
Thesis Advisor

Gamani Karunasiri
Second Reader

James H. Luscombe
Chairman, Department of Physics

THIS PAGE INTENTIONALLY LEFT BLANK

ABSTRACT

The goal of this thesis is to explore the utility of in-situ optical imaging of charge transport imaging in multi junction solar cells. An in-situ measurement of a manufactured solar cell's key material parameters is difficult. Many sophisticated models may be used to predict performance of new cell arrangements and suggest next generation improvements. In parallel, an experimental view into a complex, multi layered, alloyed semiconductor device can provide important feedback for material growth and device fabrication.

This body of work builds on the previous work of extracting estimated minority carrier diffusion lengths from multi junction solar cell materials. Indium Gallium Phosphide double heterostructures have been investigated previously with effective results. A technique to estimate electron diffusion length from a luminescent sample intensity distribution has been developed.

This thesis investigates imaging transport and applying the diffusion length estimation directly in the triple junction device. Luminescence from individual layers was isolated using optical filters. The effect of varying temperature and applying bias during the imaging technique is investigated as well. A strong dependence of effective diffusion length on environmental temperature was measured. In addition, a weak dependence of effective diffusion length on bias was measured, with the effect slightly greater in the top, as compared to the central cell.

THIS PAGE INTENTIONALLY LEFT BLANK

TABLE OF CONTENTS

THIS PAGE INTENTIONALLY LEFT BLANK

LIST OF FIGURES

THIS PAGE INTENTIONALLY LEFT BLANK

LIST OF TABLES

THIS PAGE INTENTIONALLY LEFT BLANK

ACKNOWLEDGMENTS

I would like to express my sincerest gratitude for Professor Nancy Haegel and her professional guidance in my thesis journey. Her technical expertise, and above all, her unflappable inspiration and never ending patience were valued assets throughout this work, especially with the JOEL scanning electron microscope that provided most of my data. I enjoyed the never-ending assistance I received from her. I extend many thanks also to Professor Gamani Karunasiri for his assistance in my investigations.

I thank Dr. Hojun Yoon of Spectrolab for providing new and exciting prototype solar cell samples for me to experiment upon. I also thank Mr. Mike Talmadge for the process of Lextract correction that he previously developed which was used to estimate key properties of the materials I investigated.

Finally, I thank the Naval Postgraduate School Physics Department for my excellent academic instruction.

THIS PAGE INTENTIONALLY LEFT BLANK

I. INTRODUCTION

A. PURPOSE OF THESIS

Many new technologies and materials are being developed and evaluated in the attempt to achieve improved efficiency solar cells. The need to move forward on these improvements is driven by the increasing price of oil and other traditional fuels, the cost of traditional solar cell materials, and the inherent large surface area of solar cell surfaces required for large power applications.

Many possible solar cell improvements are being investigated, including new materials and alloy combinations in multi junction cells. The analysis of any improvement in material in a high efficiency multi-junction cell can be difficult to mathematically model, and much effort is involved in preparing physically representative samples of complex new cell prototypes. Techniques are required to provide relevant information at various stages of device development.

Resistance, electric potential, current flow, charge mobility, and other parameters can vary throughout localized regions of the many differing layers of a cell. The complex semiconductor layers of a triple junction solar cell can create widely varying values of key performance parameters. This leads to complex overall parameters of a cell. The direct knowledge of the cell's transport parameters at various locations within a cell prototype can help determine what in the cell is improved and why, and therefore how to improve further.

This thesis explores techniques for extraction of localized performance parameters of a manufactured experimental solar cell. These techniques can evaluate new solar cell prototypes, so that, direct evidence of localized performance can be obtained and used to refine further choices for improvements. These techniques can also be used to understand cell performance degradation over the lifetime of a cell.

B. MILITARY RELEVANCE

Most equipment that operates in space uses high efficiency solar cells. The solar cell's size and weight are always the major factors concerning the feasibility and the cost of placing such hardware in orbit. This also includes electrical power output degradation over time. These concerns are just as important for military applications as they are for non-military applications. The military also is researching the development of many other terrestrial power applications that are self-sufficient, which possibly could operate from cheaper solar cells vice more expensive, life limited battery packs. These applications could benefit as well from the improvements in cost, size, weight, and efficiency of solar cells.

Military equipment in space is subject to a harsh radiation environment. By design, solar panels on space units will face the sun, fully exposed to the sun's damaging radiation, as they are not protected by the shielding effect of the earth's atmosphere.

C. THESIS OVERVIEW

Chapter I, the introduction, discusses why new techniques should be employed to directly evaluate solar cell prototypes with new material or designs for key performance parameters. An evaluation of the diffusion lengths of minority carriers, which in a solar cell layer of p-type material would be electrons, provides an important characteristic of the cell junction's performance.

Chapter II, the background, explains the basic construction of a triple junction solar cell, the description of electron diffusion length, and how transport imaging is used to directly estimate the electron diffusion length. Previous work on obtaining electron diffusion length information from solar cell materials is reviewed.

Chapter III, the experimental approach, describes the equipment and solar cell prototype samples used for the investigations in this thesis. The chapter also reviews optical filtering options and presents the mathematical approach to obtaining electron diffusion length information from the data.

Chapter IV, the diffusion analysis, discusses the data extraction techniques for this investigation. The optical intensity profile of the solar cell sample CF3 is shown and the analysis of CF3 in multiple bias conditions is described.

Chapter V, the alloy and bias analysis, presents the results derived from the data. The goals of this thesis work are to explore the extraction technique for electron diffusion length selectively upon particular junctions within a manufactured prototype triple junction solar cell, study the effect of bias on transport imaging in the prototype cell, and compare the results of varying Aluminum fraction in the prototype cell design with an AlGaInP top cell.

Chapter VI, the conclusion, examines the results. In this thesis, the use of an optical filter or optical filters was used to isolate the analysis to specific semiconductor junctions in a new design prototype triple layered cell. This experimental solar cell design allowed the testing the effect of varying the Al alloy concentration on electron diffusion length. In addition, the solar cell was biased during analysis to study the effects of electric field electron drift on the luminescence distribution.

THIS PAGE INTENTIONALLY LEFT BLANK

II. BACKGROUND

A. TRIPLE JUNCTION SOLAR CELLS

1. Efficiency Considerations

Many different competing technologies exist concerning solar cell design and material selection. Solar cells that operate at the highest efficiency to date are normally in a triple junction (tandem) arrangement. A single cell solar cell is not able to efficiently absorb all the wavelengths of the photons received from the sun. A solar cell's wavelength absorption range is limited to only a portion of the solar spectrum based on limits of the material's energy bandgap. The bandgap energy (E_g) is the minimal but necessary energy exchange for an electron to transition between the valence band and the conduction band. When photon interactions that produce free carriers in the material occur at energies above the material's bandgap energy or energies, energy in excess of the bandgap is primarily absorbed as heat.

In a triple junction cell, solar radiation penetrates the surface of the triple junction cell and continues through three separate but adjacent layers before reaching the bulk substrate material. A cell's overall efficiency can be increased significantly when three cells are placed together and absorb different regions of the spectrum to provide an active cell volume that can facilitate maximum absorption of the penetrating electromagnetic radiation. Multi-cell arrangements have two or more junctions, and the high efficiency cell designs today are commonly found to consist of three cells layered on top of each other.

Currently, the conversion of solar power to electrical power efficiency for an innovative design triple junction solar cell is up to about 40% [1]. Spectrolab Inc. currently markets a ($GaInP_2$/GaAs/Ge) Ultra Triple Junction Solar Cell with a beginning of life (BOL) average efficiency of 28.3% at maximum power [2]. The relatively cheaper commercial amorphous silicon crystal single junction cells are

high as 13% [3]. The manufacturing techniques are now becoming more and more sophisticated as material costs are about 70% of total manufacturing costs [4]. Three junctions are generally sufficient, with the right composition of cell materials and dimensions, along with careful semiconductor doping and other manufacturing treatments, to create a high efficiency solar cell that can absorb the majority of the incident photon radiation.

2. Construction

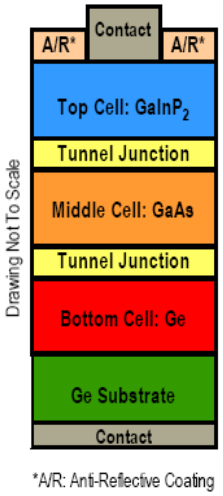

Figure 1. Example of a simplified triple junction layout [From 2].

The typical triple junction cell layout has three cells: a top cell, middle cell, and bottom cell of different semiconductor materials, generally with a tunnel junction separating the cells. The multi-layers of a cell are typically grown on top of a relative thick substrate material, which is usually of similar material to the bottom most cell junction layer. Figure 1 shows this typical arrangement for a triple junction cell. It includes an anti-reflection coating that improves the external quantum efficiency (QE). Electrical contacts are shown and provide current flow to the external circuit. The two tunnel junctions are in the tandem arrangement to allow electron flow to the next cell junction, preventing two adjacent cells from forming a barrier to the current flow.

There are significant efficiency issues that affect the capability of each cell to convert its absorbed photon radiation into electric potential and provide electrical current in a balanced cell tandem. For example, a solar cell's junction nearer to the surface than those farther away may be thinner as these layers receive more light and all cell layers need to operate with the same electrical current. The cell junction's layer thickness is typically determined by the cell's electron and hole transport properties. Internal series resistance also significantly limits choices and dimensions of materials used.

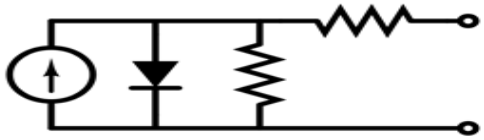

Figure 2. Schematic of an individual cell's non-ideal electrical equivalency.

The equivalent circuit of single cell is shown in Figure 2. Each cell has a series resistance due to the inherent resistivity of the materials and also has a parallel diode function and shunt resistance. The diode passes current in reverse within the cell, representing the cell's internal electron and hole recombination.

Inside the cell, there is a p-n (p-type/n-type) semiconductor junction. A n-type semiconductor is doped with a donor impurity to cause creation of free electron concentrations in the semiconductor leading to conductivity. The p-type semiconductors are doped as well, but with acceptors to create conducting hole carrier concentrations instead. An isolated p-n junction generates a built-in electrostatic potential: The n-type material diffuses high electron concentrations from atoms within a certain distance to the barrier of the p-type material into the p-type hole rich volume. These electrons in turn populate orbits in atoms in the p-type material within a certain distance to the n-type material barrier. The difference in concentrations of charge density within these two co-located regions creates a local electric field. This electric field that was created by the charge

density gradient will then correspondingly balance the diffusion, or in other words, an electron drift will be established that will be equal and opposite to the electron diffusion. The electric field creates a difference in the electrostatic potential across the junction.

This built-in electrostatic potential can create a ‘photovoltage’ across the cell because of photon interactions that generate additional free carriers. If the n-type material thickness is close to the (average) hole diffusion length and the p-type material thickness is close to the (average) electron diffusion length, holes generated in the n-type material will diffuse to the p-n junction, rather than recombine with generated electrons in the n-type material. The excess electron generation rate over recombination rate provides a current flow, which is then distributed between the internal diode function of the junction, the internal resistance of the junction materials, and any external circuit connected to the cell.

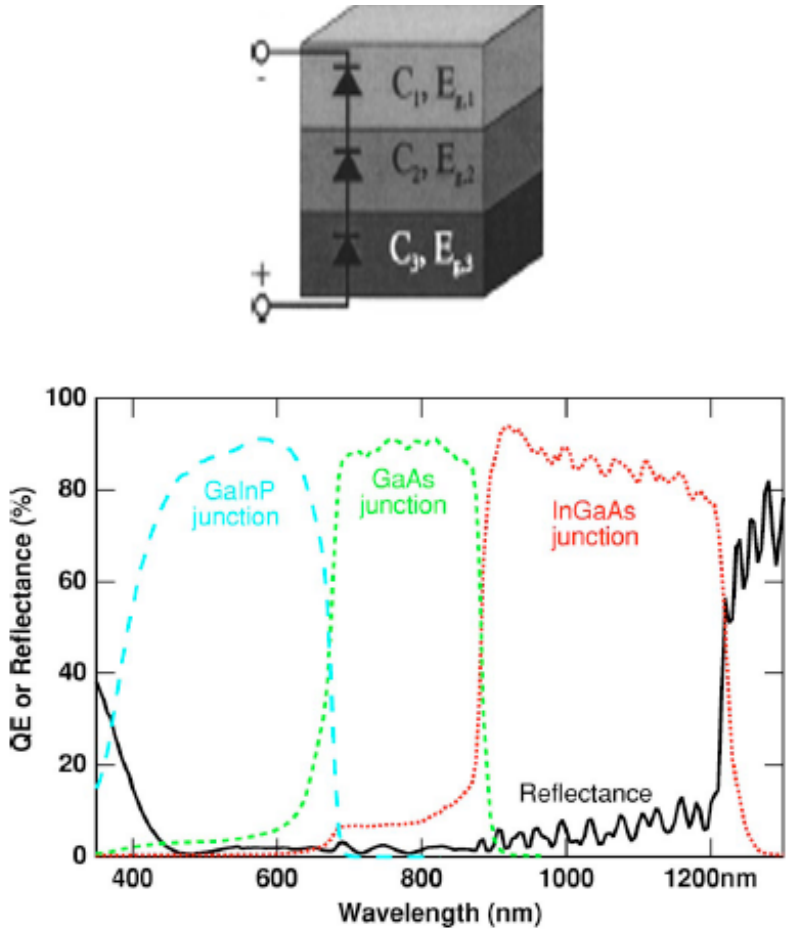

Figure 3. An example of a simplified triple junction layer and its QE performance over wavelength [After 5].

A typical triple junction cell as shown above in Figure 3 demonstrates how, with an ensemble of three different cells, the QE could be optimized throughout the solar wavelength spectrum. This particular triple cell happens to be a combination of specific III-V semiconductor materials grown epitaxially. However, many other cells being produced or in development are built with other combinations of cell layer materials.

3. Ongoing Research

Research is ongoing in the solar cell industry, investigating improved manufacturing and materials to overcome rising energy and material costs and to

improve upon numerous solar cell size and weight restricted applications. The multiple variables in potential improvements are difficult to model fully. Manufacturers must test new formulations of cell materials and new manufacturing techniques. Less expensive solar cells may also be made from many materials other than semiconductors. UC Berkeley has reported a new cell technology made from plastic based on inorganic nanorods and semiconducting polymers that can be painted on surfaces that is relatively cheap compared to other solar cell materials. These early designs so far have an efficiency of only 1.7%, but some project that improvements to this technology could lead to efficiencies of up to 10% [6]. However, high efficiency solar cells are currently all based on semiconductor multilayers.

Space based applications demand solar cells of the highest efficiency, lowest weight and most resilient to environment effects such as radiation exposure. A 'radiation hardened' solar cell degrades less over its lifetime of operation in space and therefore can be made smaller and still deliver the required power at its end of life. Therefore, radiation hardening solar cell research also requires exploration into various new types of solar cell materials and designs. High-energy electrons and protons in space will irradiate the cell materials and can ionize the atoms such that atomic displacements occur, changing the lattice structure of the cell and causing local defects.

As the development of new materials and designs moves forward, the need to apply techniques that can rapidly characterize the performance of these new solar cell materials and designs becomes very important. Material parameters such as electron mobility and diffusion length are key indicators of actual cell performance.

B. CATHODOLUMINESCENCE

Cathodoluminescense (CL) is the emission of light from a sample due to bombardment by incident electrons. The incident electrons may carry excess energy and the excitation can create additional free electron-hole pairs in the

sample. The excited carriers recombine to create photons. The distribution of this electromagnetic radiation from solar cell materials presents a signature of the electron diffusion and other parameters within the material in response to an electron beam excitation. A controlled and adjustable beam of electrons incident on the surface of a sample of solar cell material, can produce light intensity distributions that reflect relative electron diffusion and mobility characteristics. These photons emerge from the material and are detected but may be emitted at a distance away from the center of the incident beam.

The depth of the electron beam penetration and the diameter of the beam may be adjusted to affect the emission pattern. In the case of a scanning electron microscope (SEM), the electron beam acceleration voltage can be increased which would increase the depth of electron beam penetration. Increasing the current of the electrons that strike the surface (known as the probe current) would increase the diameter of the 'probe' of incident electrons striking the surface. These two parameters are important because they determine the volume over which excess carriers are created in a CL experiment.

A 20 keV electron beam can penetrate to a depth of up to 2 μm for Gallium Arsenide (GaAs) [8]. Solar cells have junction layers within this depth and can create photons when the electrons recombine. The emitted photons have energies and therefore wavelengths associated with the bandgap energy of the junction. The penetrating electrons impact and enter the solar cell surface with a diameter and cause a distribution of energetic free electrons within a corresponding volume. There is an average lifetime and associated average diffusion length of the free electrons in the material.

C. ELECTRON DIFFUSION LENGTH

The distribution of the luminescsence from solar cell materials of critical interest may present a signature of the electron diffusion that occurs within a p-type material. A free electron within the material has net motion due to drift or diffusion. Drift occurs due to an electric field gradient, while diffusion occurs due

to an electron concentration gradient. The diffusion length (L) for a particular region of volume is a mathematical average of individual electron diffusion lengths, and is given by:

$$L = \sqrt{\frac{\mu \tau kT}{e}}$$

The components of diffusion length are electron mobility (μ), electron lifetime, i.e., mean free recombination time (τ), Boltzmann's constant (k), temperature (T), and electron charge (e). The mobility is a measure of the ease with which an electron moves through the lattice:

$$\mu = \frac{e\tau_S}{m^*}$$

The mobility is affected by the electron mean free scattering time (τ_S) and the electron's effective mass (m*). The effective mass is generally different then the free electron mass. This additional mass value compensates for the lattice interaction with the moving electron. Electrons that electrostatically interact with other particles, i.e., experience force, have these contributions to motion 'hidden' in the effective mass value to forgo additional calculation terms for mobility derivation. The effective mass contribution is averaged over the population of electrons, is relatively constant throughout a homogeneous volume of a cell layer, and is therefore considered a constant like the electron's mass. The electron lifetime is the time constant for the decay of conduction electrons n_0 to n_1 in time $t_{0\rightarrow 1}$ back to their bound state:

$$\tau = -\frac{t_{0\rightarrow 1}}{\ln(n_1 / n_0)}$$

The diffusion length L is therefore primarily dependent on the lifetime, the scattering lifetime and the effective mass of the electron:

$$L = \sqrt{\frac{\tau_S \tau kT}{m^*}}$$

A solar cell that efficiently converts photons to current is generally one that has longer diffusion lengths for its minority carriers. Electrons that travel farther, due to longer diffusion length, will reach adjacent semiconductor junctions instead of recombining. When more electrons reach semiconductor junctions that have been biased to control the flow of electrons, there is more photovoltaic action in the form of more overall net electron current. Therefore, among other things the diffusion length is one of the key parameters in solar cell design and material selection. Note: these calculations apply equally well to the diffusion of holes in n-type semiconductor materials.

D. DIFFUSION LENGTH ESTIMATION

The distribution of intensity of light over the surface area due to CL would reflect the distribution of electrons generated in the material if the electrons recombined with holes where they were created. However, electrons scatter about and travel distances prior to this recombination. Although electrons may have an averaged travel distance of zero in certain circumstances, any kind of a concentration gradient will contribute diffusion in the direction of less concentration of electrons. There also could be an electric field, which causes a drift of electrons towards the negative side of the electric field as well. The effect of the concentration gradient generally leads to a flattening of the distribution of free electrons away from the center. This steady state distribution of the free electron population beyond the generation volume provides direct evidence of electron diffusion. A mathematical calculation to account for the electron population distribution, seen as photoluminescence, can be done outside the area of the incident electron beam, and as these populations must be due to electron diffusion (or drift), a measure of electron diffusion is possible.

Experiments have previously been performed to derive electron diffusion lengths using a scanning electron microscope, combined with an optical camera that can measure spatial luminescence intensity. These experiments were performed on solar cell material double heterostructures that determined diffusion effects in materials without the associated drift effects caused by semiconductor junction built in electric fields. This work examined the effects of the built in fields by measuring luminescence intensity distributions in actual triple junction cells.

III. EXPERIMENTAL APPROACH

A. EQUIPMENT

A JOEL-840A Scanning Electron Microscope (SEM) provided the base system for investigation of solar cell materials using an electron beam to produce optical luminescence in a controlled environment. The electron beam is generated by a tungsten hairpin filament and can be controlled via its accelerating voltage and the probe (i.e., incident electron) current. It produces a buried sphere of free electrons extending to a depth of up to 2 μm for a 20 kV accelerating voltage setting based on the atomic numbers of 31 and 33 for Gallium Arsenide (GaAs) [8]. The probe diameter in our system has been experimentally determined to be 0.163 microns FWHM if operated with a probe current of 1×10^{-9} amperes at 30 kV accelerating voltage [9].

The region of minority charge carrier generation leads to an emission of light in certain materials. The distribution of the intensity of the illumination is dependent on the distribution of the free carriers in the buried region and the transport motion of these carriers within the material between the time of generation and their recombination to create the photons. The wavelength of the electrons for 20 kV is approximately 0.008 nm. Although the SEM routinely operates to scan the probe quickly over an area of a sample to render a secondary electron image, the beam can also be held in a fixed position in “spot mode” to create a steady state optical image of the illumination intensity distribution.

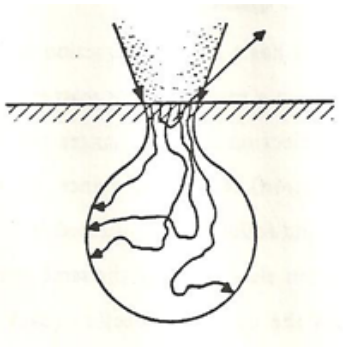

Figure 4. Illustration of a generation volume of incident electrons within a sample [From 9].

An retractable optical microscope attached to the SEM produces an image of luminescent samples on an electrically cooled, Apogee KX32ME Charge Coupled Device (CCD) camera (array). The CCD camera can record images with a resolution limit derived from its physical pixel size of 6.8 μm x 6.8 μm. The microscope then magnifies the image ~20X to a width coverage of a pixel to 0.4 μm x 0.4 μm [11]. The image captured in a data file can be profiled using several related approaches and used to determine electron diffusion characteristics. The CCD images were captured in Diffraction Limited's MicroCCD™ v3.13 image processing software. The line intensity profiles of the CCD images were then analyzed in SigmaPlot v9.01 software.

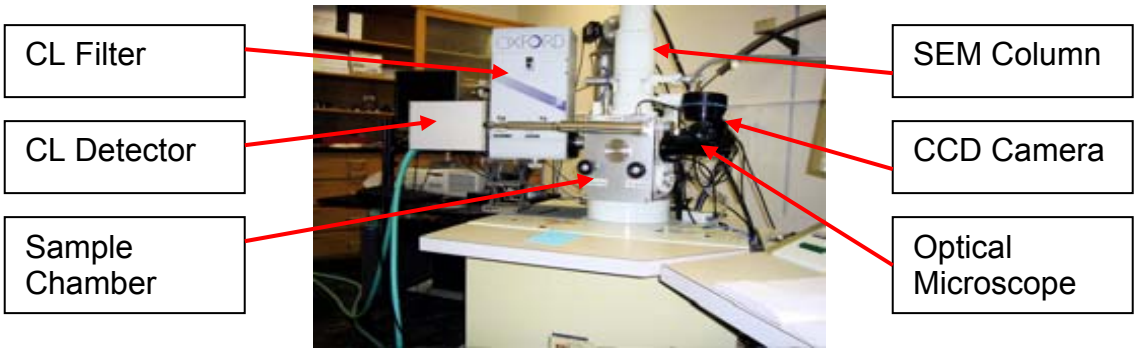

Figure 5. A photo of the JOEL SEM electron gun and its sample chamber with attachments.

Also attached to the SEM is a water-cooled Oxford CL Detector for both Monochromatic and Panchromatic analysis. The Monochromatic mode measures the intensity of illumination as a function of wavelength with a monochrometer to determine the spectra of the emitted CL. It was used occasionally to isolate illumination intensities to certain wavelengths and thereby associate the illumination with specific cell junctions that are photo luminescent at wavelengths dependent on the bandgap. The Panchromatic mode collects all wavelengths.

Although the SEM electron beam must be operated in a vacuum, an electrically isolated connection allowed a Keithley 2400 SourceMeter to apply voltage bias to a solar cell in the chamber when desired.

B. SAMPLES

Several new solar cell material samples were evaluated. Pioneer Materials produced $CuInGaSe_2$ on a substrate. The $CuInGaSe_2$ samples are CIGS1, CIGS2, and CIGS3 and had measured purities of the CIGS as listed below in Table 1.

CIGS1	Sodalime + Mo + CIGS(6N Purity)
CIGS2	Sodalime + Mo + CIGS(4N Purity)
CIGS3	Sodalime + CIGS(6N Purity)

Table 1. Compositions of the CIGS samples.

Manufactured triple layer solar cells made by Spectrolab with a AlGaInP top layer were also evaluated. The cells are labeled CF1, CF2, CF3, and CF4 and have varying percentages of Al in a AlGaInP material in the top cells as listed in Table 2. The manufacturer reported the listed bandgap energies and the photon wavelengths are calculated from them. The mid cells are GaInAs material and the bottom cells were Germanium for all four samples.

	Alloy	Bandgap	Photon λ
CF1	0 % Al	1.9 eV	653 nm
CF2	5 % Al	1.95 eV	636 nm
CF3	8 % Al	2.0 eV	620 nm
CF4	unk % Al	2.1 eV	590 nm

Table 2. The varying content of Al in each CF solar cell Top Cell.

C. OPTICAL FILTERING FOR MULTI-JUNCTION ANALYSIS

Different cells within the same solar cell structure will produce light with intensity peaks occurring at wavelengths associated with the cell's specific bandgap energies when the cell is forward biased enough to cause carrier injection and light emission. This wavelength variation can be used to selectively study transport in the different cell layers.

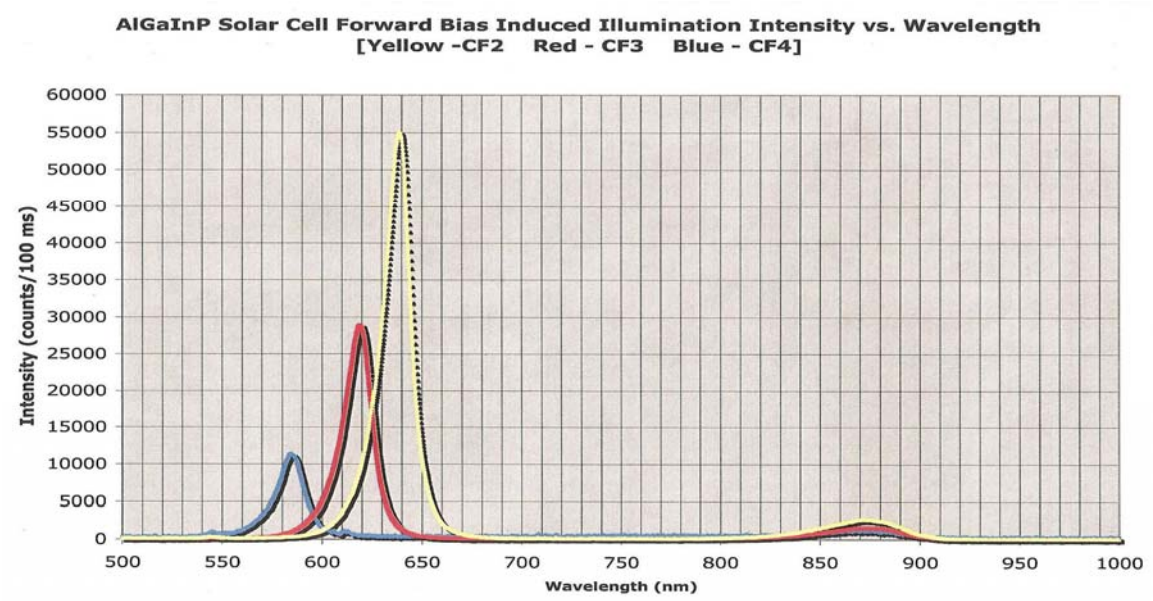

Figure 6. Forward bias CF sample cells luminescence spectrum.

In Figure 6, spectra from samples CF2, CF3, and CF4 under forward bias are compared. The samples were biased by connecting a voltage source to the solar cell and applying 2.1 Volts DC. An Ocean Optics Inc. USB Spectrometer

detected the light emitted from the cell. Although relative intensities between the samples are not absolute, it can be seen that an increase in Al content in the samples shifts the wavelength intensity peaks from 640 nm to 585 nm, while the other intensity peaks are consistent at 872 nm. These varying peaks correspond to the manufacturer's provided bandgap energy information. The middle cell peak for each sample that does not shift has a bandgap energy of 1.42 eV. This smaller E_g corresponds to the InGaAs layers.

The utility of this information is that one may now select a correct optical filter or filters that transmits only the wavelengths attributed to a certain cell junction. Glass filters with known percent transmittance over wavelength performance can be used inline to a detector to isolate individual cell's junction emission. Figure 7 below shows an example of a bandpass filter that has a similar transmission function to what was used in optical filtering performed in the experimental work.

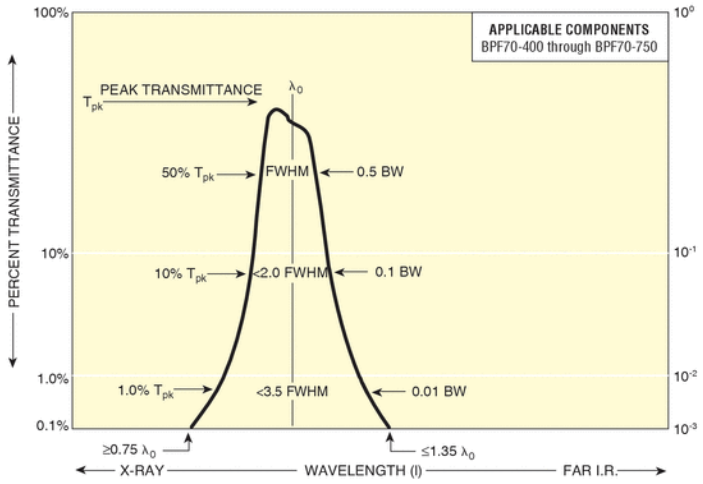

Figure 7. Example of percent transmittance for a typical bandpass filter [From 7].

For example, a bandpass filter for 600 with a window of 70±30nm FWHM for a CF3 sample would transmit only the emission, and therefore the corresponding transport information, through to the detector from the top cell. The intensity of the top cell 623 nm peak is 10 times that of the middle cell 872

nm peak under a bias induced emission, and the filter can easily remove the small middle cell contribution to the overall intensity. However, the unfiltered intensity ratio is much different for the cell if the induced emission is due to SEM electron excitation, and the use of bandpass filter is then much more important to separate the contributions to the CCD image intensity. Figure 8 shows that in CL, the mid cell emission has an approximate peak intensity of 250x above the top cell peak emission.

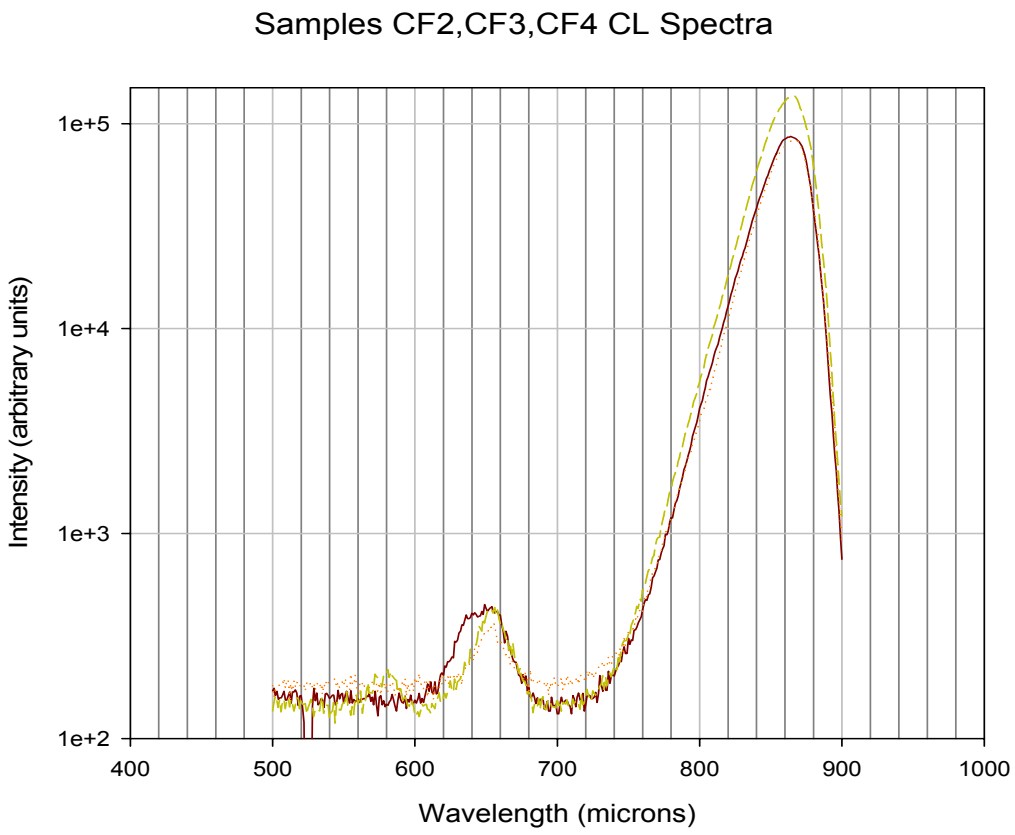

Figure 8. CL intensity as a function of wavelength.

D. DIFFUSION LENGTH EXTRACTION

1. 1/ Slope Technique

An approach has been developed to estimate a material's electron diffusion length from an image of light from the recombination of minority carriers. The key information is contained in the slope of the spatial decay of normalized light intensity of a CL emitting solid under spot mode excitation. As the decay in intensity is measured along a straight line distance from the center of an electron carrier generation point, that decay beyond the electron generation region is subject to the radial spreading of diffusion and any drift of electrons. The following equation calculates the intensity variation in the x-direction given a radial symmetric x, y diffusion and x-direction drift, but with no diffusion or drift in the z-direction, given a two dimensional Gaussian shaped charge generation region [11]:

$$I_{ss}(x) = \frac{gn}{2L^2\pi^2}\int_{-\infty}^{\infty}\int_{-\infty}^{\infty} e^{-\left[n\left(\eta^2+\xi^2\right)\right]} e^{\left[S_x(x-\eta)/2L^2\right]}$$

$$\times K_0\left(\frac{\sqrt{S_x{}^2+4L^2}}{2L^2}\sqrt{(x-\eta)^2+\xi^2}\right) d\eta\, d\xi$$

In the above equation, L is diffusion length. S_x is the electron drift length in the x direction, g is proportional to the electron generation rate, n is inversely proportional to the standard deviation of a Gaussian approximated electron generation region, and η and ξ are the integration variables for x and y respectively. The above equation contains a zeroth order modified Bessel function of the second kind that approximates the I_{SS} (steady-state intensity) in a one dimensional intensity line of values along across the x direction from the center of the peak. The Bessel function can be approximated by an exponential decay to a good approximation when x > L. Simulations have shown that this approximation is within 10% for x > ~5L [11]. Note that the above equation does

not calculate any impact on L due to electric fields that have a z direction component such as those that are naturally found in the various junctions of an actual solar cell device.

Without any applied electric fields, and when more than 5 diffusion lengths away from the peak and outside the radius of the generation volume of electrons, the distribution can be further approximated to $I = I_{SS}(x) \approx I_0 e^{-x/L}$. Therefore, if L is constant, then using mx = y + b, we have: y = $Ln(I)$ and m = $-1/L$. With experimental variance in I over x, a linear regression of an array of an '$x, y = Ln(I)$' data plot over a range of x can yield a $-1/L$ value providing an estimate of the diffusion length.

2. $L_{extract}$ Correction

An improvement to this estimation of diffusion length can be performed by comparing derived estimates to known L values and mapping a correction factor when x is not >> L. It has been shown that for this estimation technique L will be underestimated, and there are mathematically reproducible ratios between estimated and real diffusion lengths for specified L and x/L ratios. I will use the following 'L' notations to distinguish the different diffusion lengths:

$$L_U = \frac{-1}{LR, Slope\left(Ln(I_i)/x_i\right)}$$
$$L_C = Lextract\left(L_U, x_C\right)$$

L_u is the uncorrected diffusion length, *LR,Slope(y/x)* is the linear regression of the slope of y/x and L_c is corrected diffusion length, from *Lextract(L_u,x_c)* that produces a corrected L from a given L_u and x_c. The x_c is the distance between the mid position of the linear regression of slope took place to the intensity peak. *Lextract(L_u, x_c)* is a spline algorithm in a previously created

Matlab code called $l_{extract}$ which I could use to improve my diffusion length estimations. The $l_{extract}$ correction compensates for when the Bessel function is not as well described by the exponential decay.

Although the $l_{extract}$ correction will improve an estimate of the diffusion length in a simplified cell heterostructure, that confines carriers in the layer, the improvement of the accuracy of the measurement of diffusion length in a real cell geometry that has built in electric fields, will probably be overcome by other effects also not taken in account by the estimation. Normally the $l_{extract}$ correction in materials of L < 10 μm is not large anyway, because other effects that effect the distribution are present near the generation region.

3. CIGS Cell Diffusion Length Temperature Dependence

An investigation of temperature dependence on the estimated diffusion length of a simple CIGS cell was performed. The results are shown in Figure 9.

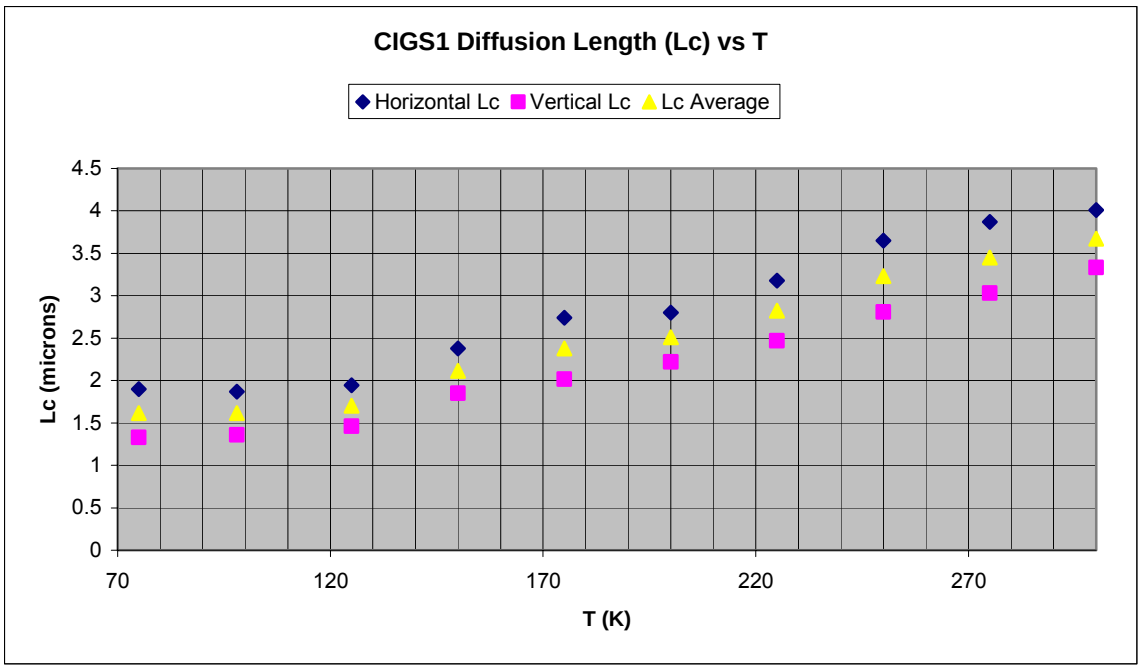

Figure 9. Temperature effect on CIGS1 Cell Diffusion Lengths.

In this cell, lowering the temperature 200K below ambient room temperature reduces the diffusion length measured values by at least half.

Using the 1/Slope technique on the CIGS samples, additional luminescence was noted within the intensity distributions that would cause inaccuracies in the diffusion length estimations. Further work is required to separate the luminescence from the relatively low emission CIGS layer from the substrate. Therefore, further work is required to confirm the diffusion length values.

There is a strong temperature dependence on the ambient temperature and this must be taken into account when evaluating solar cell materials. Certain cell applications in space may operate in low temperatures while terrestrial applications may operate between hot and warm temperatures depending on weather variations.

IV. IN-SITU TRANSPORT ANALYSIS OF A PROTOTYPE TRIPLE CELL

A. CF TRIPLE CELL EVALUATION

Four developmental 'CF' triple junction AlGaInP/InGaAs/Ge solar cells with a AlGaInP top cell were analyzed by transport imaging at different externally applied voltage bias values. This is done to study the effects on diffusion length due to varying bias as well as varying Aluminum concentration.

A 700 nm Short Wavelength Filter, i.e., a Low Pass Filter, was placed in front of the CCD camera to block the middle cell junctions emission above 700 nm. Two perpendicular cross sections of intensity values as a function of position in the 0°/180° and 90°/270° directions are obtained from the MicroCCD software and exported into SigmaPlot software for data analysis. The two cross sections are both selected through the maximum of the intensity distribution. The 0°/180° cut could be considered horizontal within the software data capture sense but it is not necessarily reflective of any particular angle relative to the sample or its environment. The 90°/270°, or vertical, cut is simply rotated 90° from the horizontal cut. An illumination intensity distribution with a forward bias of 0.5 volts was recorded by the CCD Camera and is shown in Figure 10. The graph in the top half of Figure 10 shows the horizontal distribution of intensity spot. The SEM was operated at an accelerating voltage of 20 keV and a probe current of 1×10^{-9} amps and so the approximate 0.16 micron diameter of the incident electron beam would be approximately one third of a CCD pixel dimension.

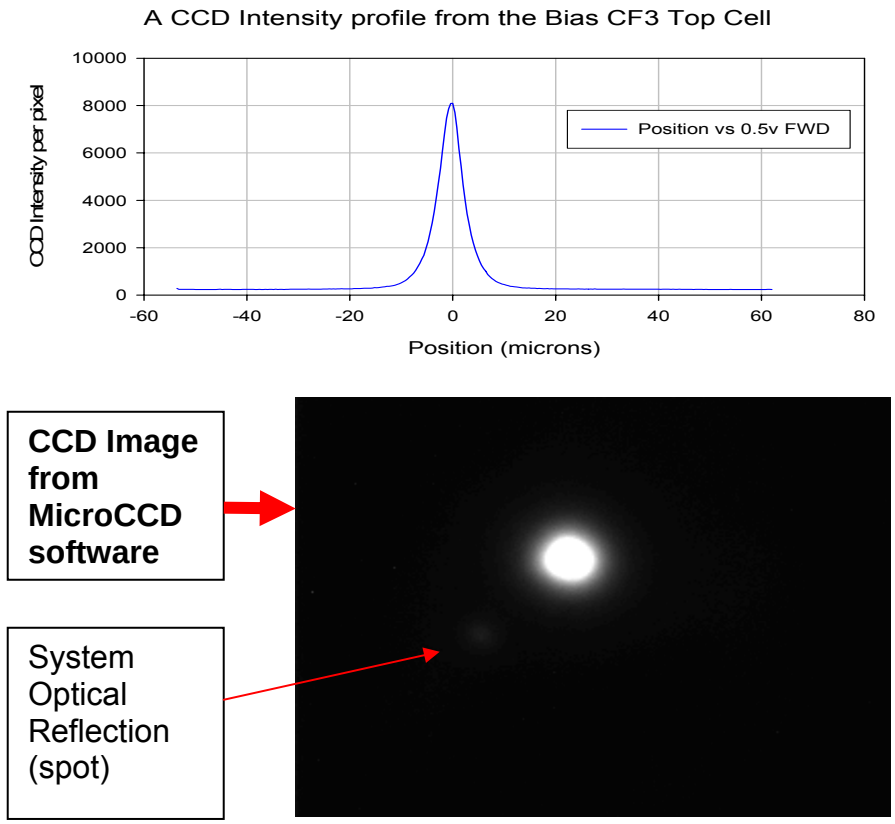

Figure 10. CCD image of a CF3 Top Cell spot with corresponding 0°/180° (horizontal) cross section line of Intensity values through the peak of intensity.

In the Figure 10 CCD Image, a small optical system secondary image appears due to a reflection in the optical train. It is an artifact, but has no appreciable effect on the data obtained. Many luminescence images were captured for a range of voltages from -2.1 to +1.7V.

The upper integer limit of the individual CCD pixel intensity recording is 10000. Various lengths of exposure time were used to place the intensity of the peak between values of 7500 and 9500 per pixel. This is high enough to obtain the best signal to noise ratio and low enough that the intensity of 10000 per pixel limit does not saturate the peak value and distort the shape of the distribution.

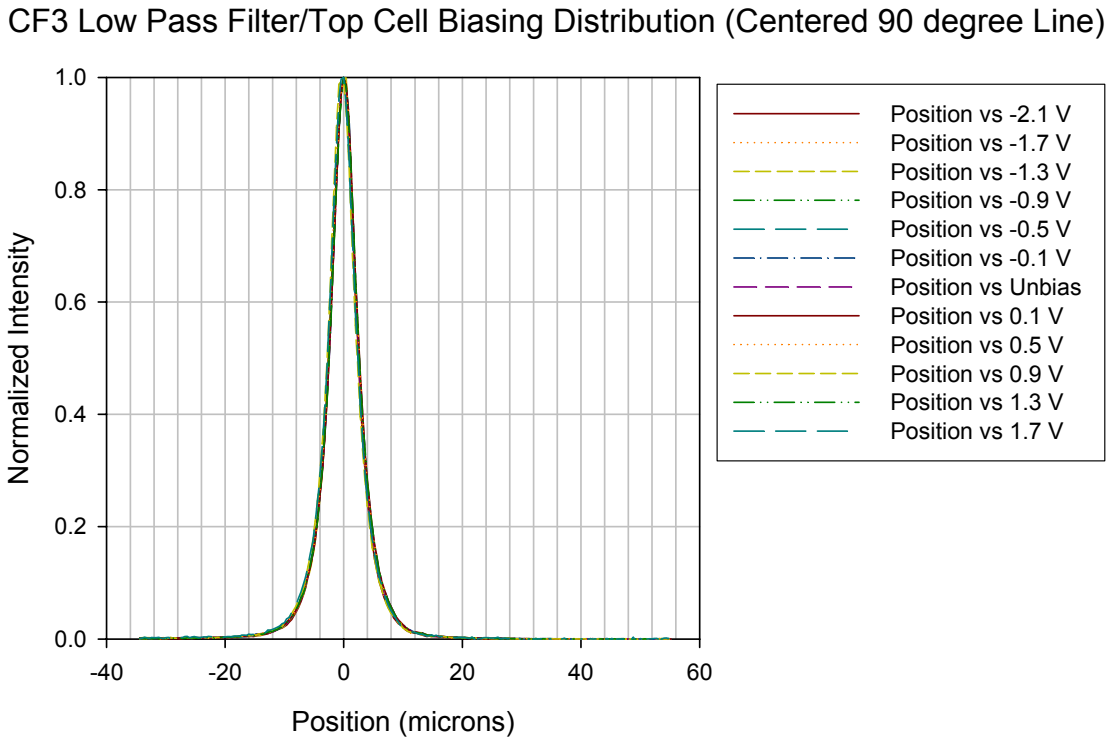

Figure 11. Top Cell normalized intensity distribution for bias voltages from -2.1 to +1.7V.

Figure 11 shows the normalized intensity (I_{Norm}) distribution of luminescence from the CF3 solar cell with different voltage bias sampled over an arbitrary straight line through the center of the peak of intensity, where

$$I_{Norm} = \frac{I - I_{Noise}}{I_{Max} - I_{Noise}}$$

Multiple images were taken over a bias range from -2.1 to +1.7V. The background noise for most images was an average intensity of about 240 to 280 per pixel and is slightly noticeable in Figure 10, but very apparent in Figure 12, where the same data are presented on a logarithmic scale. As required for diffusion length extraction, the normalized intensity peaks are then analyzed in the common logarithmic y-axis format. The semi-log slope of the lines is used to

determine where in position, slope data can be analyzed. The previously discussed approximation: $I_{Norm} \sim I_{ss} \sim K_0(r/L) \sim \exp(-r/L)$ when $r > L$, is now applied across the appropriate range of data for each side of the peak.

In Figure 12, data are useful beyond the diameter of the generation region, but not beyond where the intensity that is due to the recombination luminescence is comparable to the noise of general background light in the SEM chamber. Figure 12 shows how the background noise begins to degrade slope information beyond 12 μm from the center position. In addition, the slope appears to be gradually changing beyond 12 μm from the center. This is due to the small intensity of the cell's emission, which is low enough compared to the level of light scattering in the SEM chamber which normalization cannot correct.

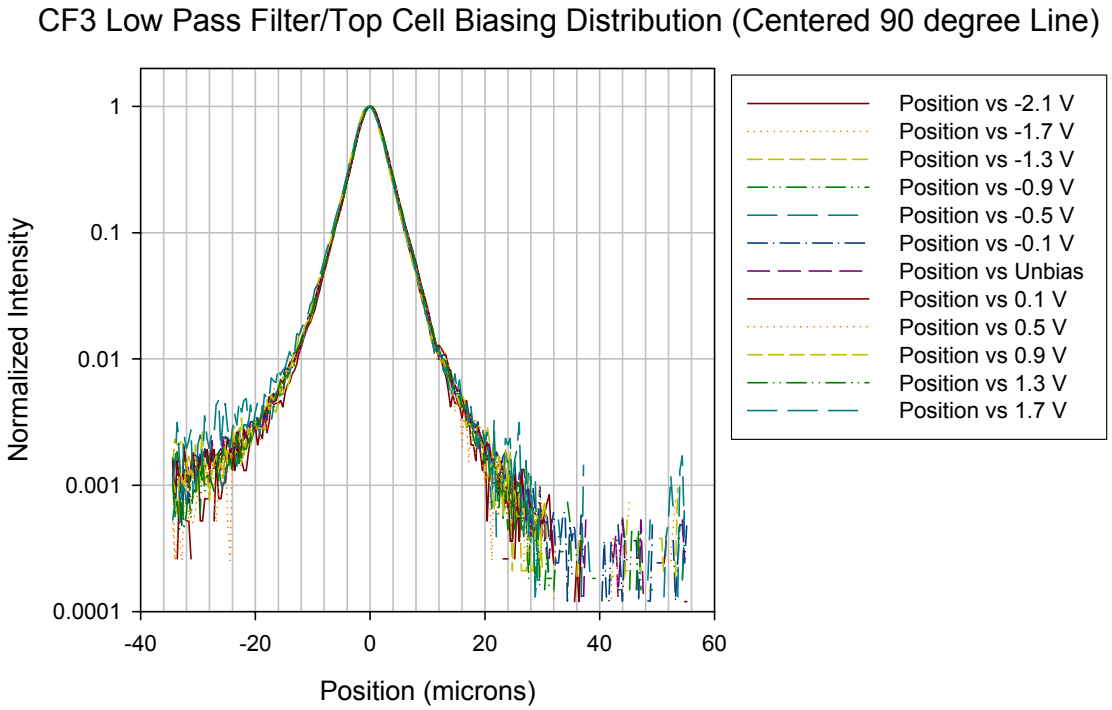

Figure 12. Top Cell normalized logarithmic intensity distribution for bias voltages from -2.1 to +1.7V.

Each line of data provides two slopes. One was on the positive position side and the other on the negative position side. The vertical lines of Figure 12 data were analyzed between the positions of -10 to -2 μm and 2 to 10 μm. The horizontal data were analyzed between the same position values. The negative slopes were inverted to obtain an uncorrected diffusion length (L_u = -1/m). The L_u and corresponding average position of the slope (x_c = -6 or 6 μm) were fed into the lextract program to return a corrected diffusion length (L_c). The four quadrant L_c values were averaged for a cell and used for bias effect comparison. The results are analyzed in Chapter V.

THIS PAGE INTENTIONALLY LEFT BLANK

V. ALLOY AND BIAS EFFECT ANALYSIS

A. VARYING ALUMINUM FRACTION TOP CELL MEASUREMENTS

Uncorrected diffusion length measurements of the CF1, CF2, CF3, and CF4 solar cells were determined by the 1/slope technique. The calculated diffusion lengths are shown in Table 3. Each sample L_u value shown was averaged from twelve values from three different spots on the surface of each sample that were further averaged for the diffusion length slope in the four perpendicular directions of each of the three profiles. Looking at Table 3, there is no visible direct relationship found between Aluminum fraction and the extracted L_u. In addition, as expected, there is no variation shown for the middle cell L_u, as there was no composition change in that cell junction.

	Al Alloy	Top Lu (μm)	Mid Lu (μm)
CF1	**0%**	0.80	1.9
CF2	**5%**	0.75	2.0
CF3	**8%**	0.80	1.8
CF4	**unk%**	0.84	

Table 3. The Al alloy variation effect on Top and Mid Cell electron diffusion measurement.

B. VARYING BIAS ALUMINUM ALLOY TRIPLE CELL

Corrected diffusion length measurements of the CF3 solar cell were determined by the 1/slope technique combined with the $I_{extract}$ correction. Those diffusion lengths values each were calculated and averaged over the four perpendicular directions and are shown in Figure 13 over a range of different bias voltages. Of particular note is the relatively weak but noticeable effect of the electric field bias on the diffusion profiles.

One explanation for the weak dependence of diffusion on bias voltage is that there is varying electron drift perpendicular to the plane of the semiconductor

layers that is caused by the change in strength of the built in fields of the solar cell. These electric fields, due to the construction of the multiple n-type and p-type junctions are decreased in layer depth with the application of a forward bias. The measured electron diffusion lengths may be increased if the magnitude of the electric fields due to the internal depletion regions are decreased. This results in less electrons moving in the z direction with less junction recombination and therefore more net more translational motion and a larger measured L_c.

The application of a forward bias increases the corrected diffusion length and therefore most likely increases the measured electron diffusion length in the plane of the layer. This includes a reduction when a reverse bias is applied. The linear regression of the data of Figure 13 gives an increase of corrected diffusion length of 0.043 microns per volt, which is a 1.3 % increase in L_c per volt.

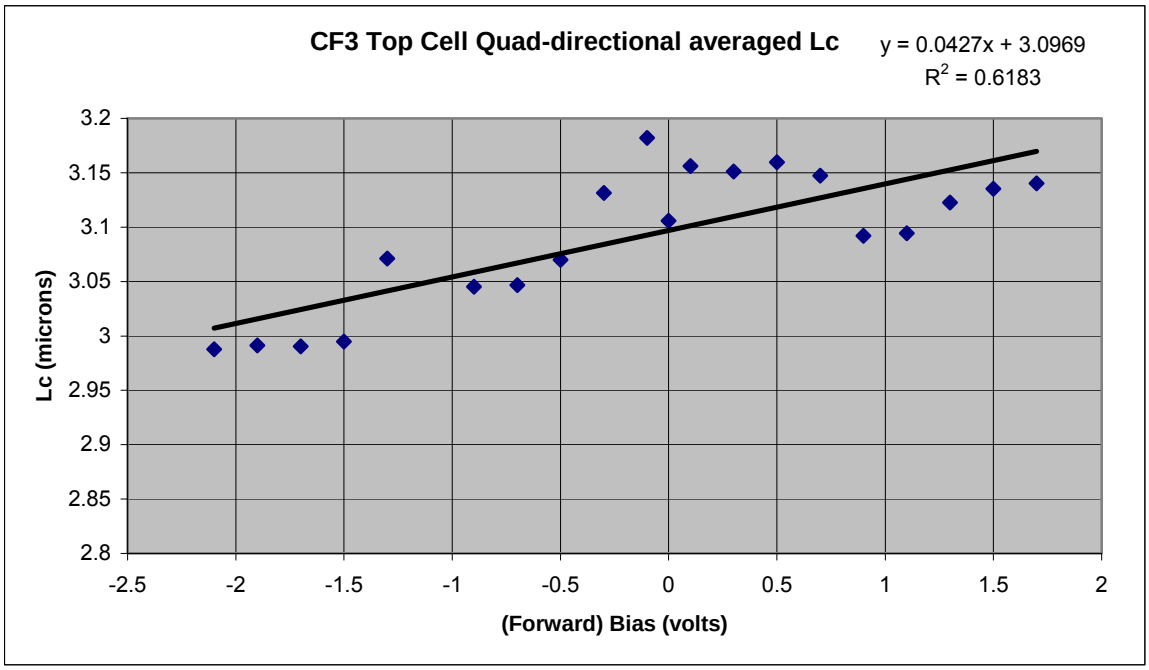

Figure 13. Bias voltage effect on Top Cell electron diffusion measurement.

This small change of the diffusion length due to an applied bias voltage shows that the strong internal electric fields are not easily affected by the bias. Therefore, the application of a forward bias during the use of this diffusion length extraction technique is not sufficient to achieve a condition to provide diffusion in the plane reflecting the actual material properties. This can be seen by comparing the length values extracted here for the InGaAs cell to the ~10 to 20 μm values that have been measured in previous heterostructures [12].

Using a filter to isolate the middle cell information, data were compiled for CF3, of with the results of the diffusion lengths averaged over four quadrants for a few different bias voltages. Figure 14 shows similar results to Figure 12 except that the peak is now flatter at the zero position. The slope analysis positions for this data was further out from the center than the top cell, between the positions of -12 to -4 μm and 4 to 12 μm.

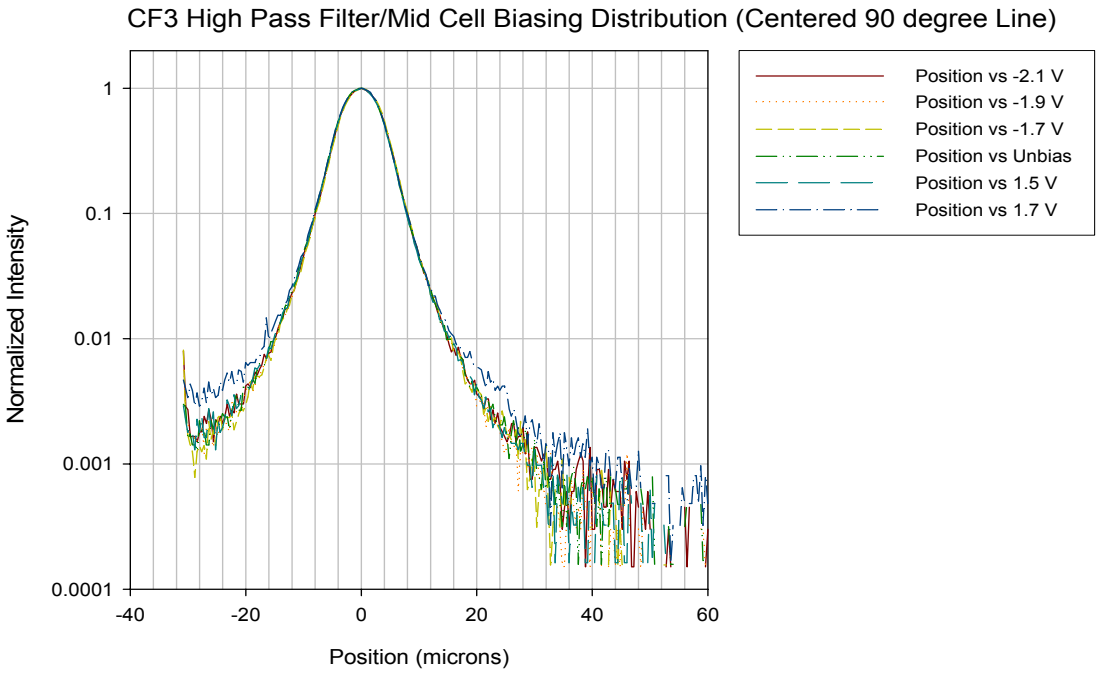

Figure 14. Mid Cell normalized logarithmic intensity distribution for bias voltages from -2.1 to +1.7V.

The flatter peak is more than likely due to the electron beam having more spreading upon deeper penetration into the solar cell material past the top cell, effective by making the real distribution of carrier generation flatter than the assumed Gaussian shape. Per Figure 15 results, the corrected diffusion lengths for the middle cell were found to be slightly lower than the top cell and the slope is shallower, only approximately 0.013 microns per volt, which is a 0.4 % increase in L_c per volt.

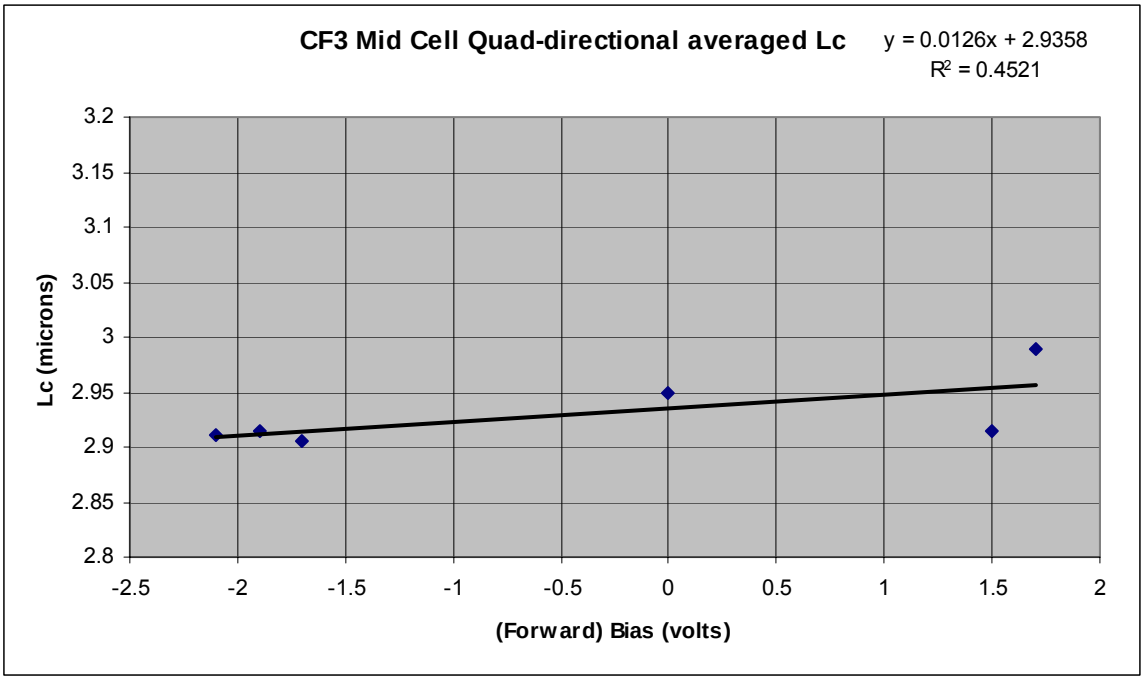

Figure 15. Bias voltage effect on Mid Cell electron diffusion measurement.

The CF3 middle cell corrected diffusion length measurements were more weakly affected by a bias. The results suggest that the deeper internal built in fields of the solar cell are less influenced by an applied bias to the cell.

C. CROSS SECTION EVALUATION OF THE CF TRIPLE CELL

An initial investigation was made of a cells CL from its cross section. The CF3 cell was set on a vertical side of a mount block in the SEM. A clean break was exposed toward the SEM column and imaged with the CCD camera.

The cross section line intensity CL of the CF3 cell with a varying bias across its layers is shown in Figure 16. The addition of a reverse bias on the cell creates no noticeable change in the intensity distribution. However, the peaks of intensity at the cell junctions are higher under forward bias of 2.0 volts due to electroluminescence.

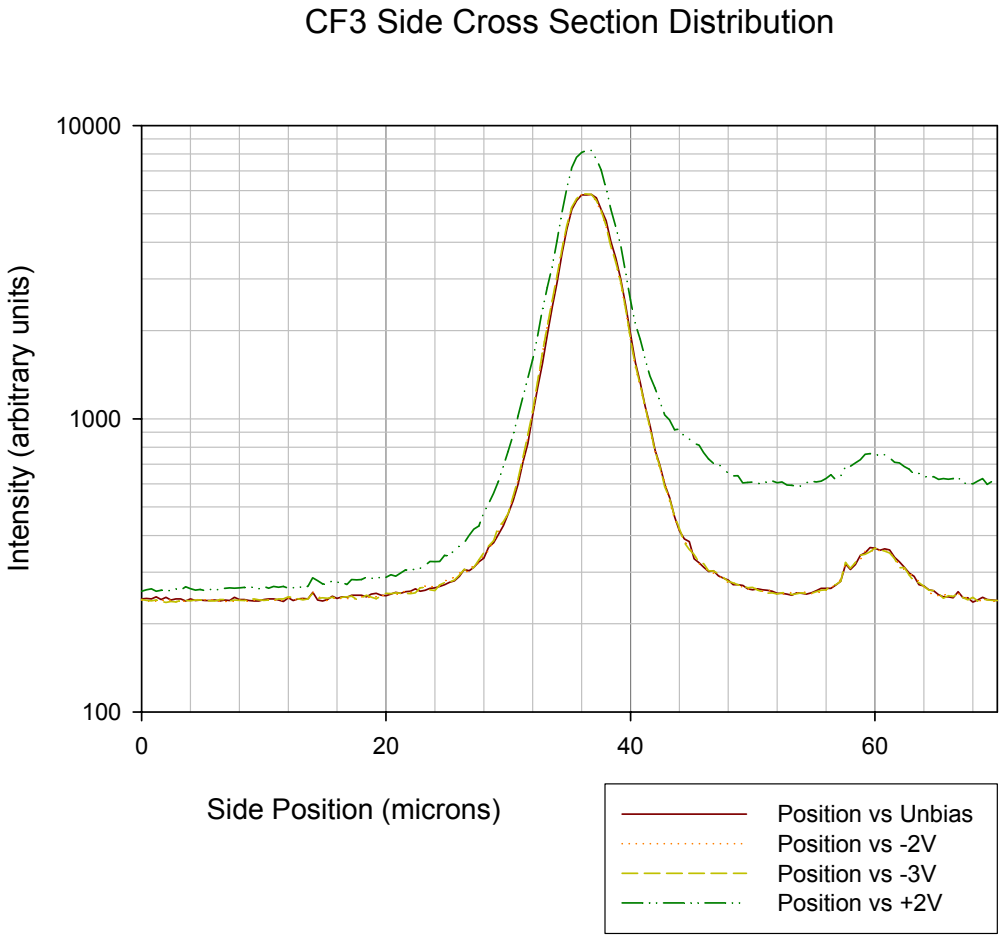

Figure 16. Bias voltage effect on a cross section of the CF3 solar cell edge.

The cell's surface illumination intensity away from the junctions is double that of the non-cell background due to the cell's material electroluminescence. The cross section shows peaks from the cell junctions on the left between positions 34 to 38 microns and a SEM chamber reflection on the right located at 60 microns. A zoom in view of the main peak of Figure 16 is shown as Figure 17 with known cell junction depths that are shown as red and superimposed onto the intensity distribution with an estimated alignment.

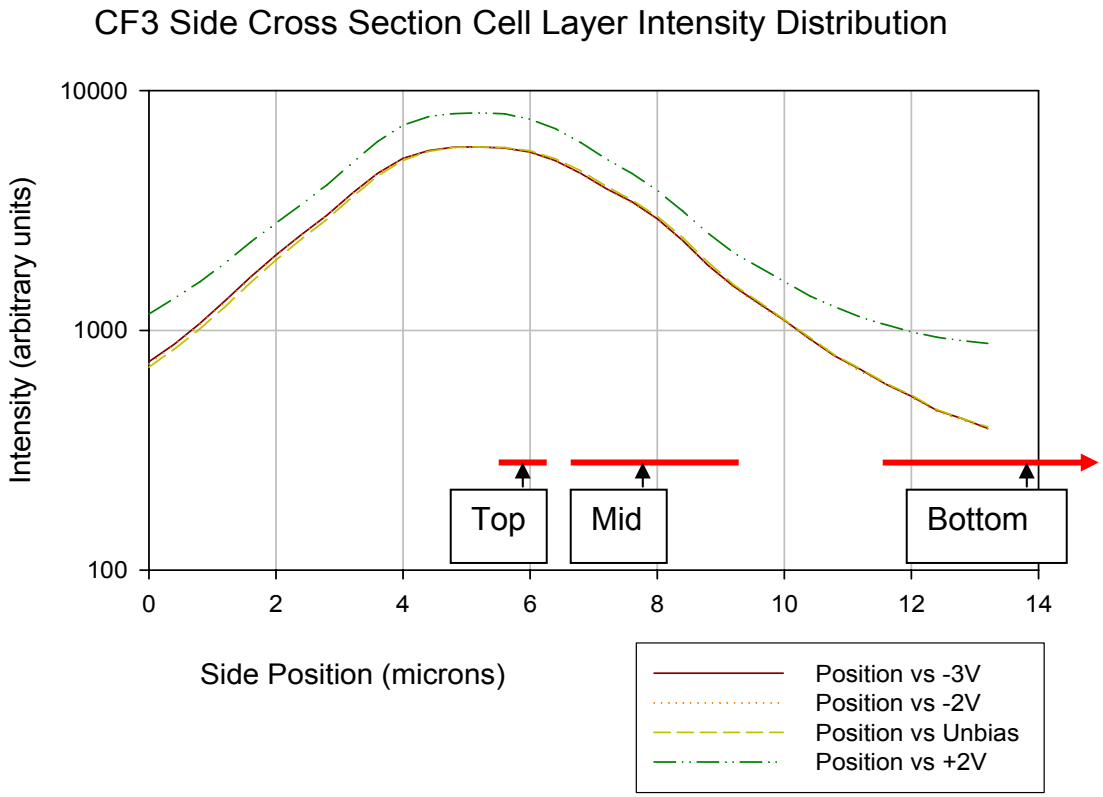

Figure 17. Close up of the CL in cross section of the CF3 solar cell edge matched to the layer depths.

A side position of 4 μm is at the top of the cell with a higher position corresponding to deeper in the cell. The figure shows that the small top cell and the top portion of the middle cell provide the bulk of the peak. There is a corresponding dip in intensity that is noticeable beyond 8 microns on Figure 17. This accounts for the transition layer material between the middle and bottom

cells. The relative layer thickness for the top, middle and bottom p-n junctions are 0.6 μm, 3.3 μm, and 175 μm respectfully. However, the depletion zones themselves within each cell are at the top side as all the top facing n-type layers are only up to 1 μm thick. The cross section resolution is limited to the pixel size of the CCD camera at 0.4 microns per pixel and the generation volume, which is comparable to the larger thicknesses of the top cell at ~1 μm. However, notice that the top side position of the top cell, which coincides with the top of the whole solar cell, has an intensity decay without material present that is nearly similar to the intensity decay to the right with further cell material present.

THIS PAGE INTENTIONALLY LEFT BLANK

VI. CONCLUSIONS

A. SUMMARY

The evidence collected in this thesis shows that the junctions of a manufactured solar cell can be individually evaluated in terms of performance parameters using optical filters. The resolution of the intensity distributions are limited by the magnification of the optical microscope and the pixel grid size of the CCD camera. This does not limit the accuracy of the 1/slope technique but can limit the capability of 'reading' the features of a multi layer semiconductor material.

The in-situ optical imaging techniques are part of a continuing, evolving effort to broaden the tools available to investigate new solar cell materials and prototypes. In the samples investigated, the electron diffusion length was estimated to be 3.1 μm for the top layer and 3.0 μm for the middle layer of the CF3 prototype Aluminum alloy solar cell. The effect of applying a bias on the CF3 cell caused changes in estimated diffusion length of 0.043 μm/Volt and 0.013 μm/Volt for top and middle cells respectfully.

B. CONCLUSION

The use of optical filtering in conjunction with the diffusion length estimation technique is effective for the isolating characteristics of specific junctions of a multi layer solar cell. The effect of temperature upon diffusion length is significant and should be taken into account when evaluating the performance of cells in a particular environment. The testing of any solar cell material or prototype should always take into account the cell's environment temperature. In contrast, the application of a bias to produce simulated operating conditions for a cell when undergoing the diffusion length estimation technique is largely not critical.

Another key result is that the accuracy of the estimation technique may not be sufficient for determination of effects due to variance of alloy concentrations in some families of solar cell prototypes. However, there could be useful applications in the study of other experimental solar cell prototypes. Further solar cell prototype research may lead to more effective applications of the estimation technique and contribute to better information for device improvement.

The solar cell industry is growing more complex and expensive. However, the potential for breakthroughs in technology that lower costs is present. The need to move forward with tools to assist in improving materials and construction of solar cells will remain high. Transport imaging can play a role in this area but further work, particularly on cross sectional techniques with higher resolution, will be required to allow for this type of characterization in actual operating solar cells.

LIST OF REFERENCES

[1] R. R. King, D. C. Law, K. M. Edmondson, C. M. Fetzer, G. S. Kinsey, H. Yoon, R. A. Sherif and N. H. Karam, *40% efficient metamorphic GaInP/GaInAs/Ge multijunction solar cells*, Applied Physics Letters 90 183516 (2007).

[2] Data Sheet, 28.3% Ultra Triple Junction (UJT) Solar Cells, Internet. Spectrolab, Inc. March 10, 2008, http://www.spectrolab.com/DataSheets/TNJCell/utj3.pdf, March 2008.

[3] J. Nelson, *The Physics of Solar Cells*. (Imperial College Press, London, 2003).

[4] Martin A. Green, *Third Generation Voltaics, Advanced Solar Energy Conversion*. (Springer-Verlag Berlin Heidelberg 2003, 2006).

[5] J. F. Geisz, Sarah Kurtz, M. W. Wanlass, J. S. Ward, A. Duda, D. J. Friedman, J. M. Olson, W. E. McMahon, T. E. Moriarty and J. T. Kiehl, *High-efficiency GaInP/GaAs/InGaAs triple-junction solar cells grown inverted with a metamorphic bottom junction*. Applied Physics Letters 91 023502 (2007).

[6] UC Berkeley Campus News Release, Internet, http://www.berkeley.edu/news/media/releases/2002/03/28_solar.html, March 2008.

[7] Specifications Page, Internet, Bandpass Filters, Newport Corporation, http://www.newport.com/store/genproduct.aspx?id=417890&lang=1033&Section=Spec, March 2008.

[8] J. Goldstein, D. Newbury, D. Joy, C. Lyman, P. Echlin, E. Lifshin, L. Sawyer and J. Michael, *Scanning Electron Microscopy and X-Ray Microanalysis*, (Kluwer Academic/Plenum Publishers, New York, New York, 2003).

[9] S. D. Winchell, *Transport in the one Dimensional Limit*, M.S. thesis, Naval Postgraduate School, Monterey, California, December 2006.

[10] JOEL JSM-840 Technical Manual.

[11] D. R. Luber, F. M. Bradley and N. M. Haegel, *Imaging transport for the determination of minority carrier diffusion length*, Applied Physics Letters 88 163509 (2006).

[12] J. Mills, *Direct Imaging of Minority Charge Carrier Transport in Triple Junction Solar Cell Layers*, M.S. thesis, Naval Postgraduate School, Monterey, CA, December 2006.

INITIAL DISTRIBUTION LIST

1. Defense Technical Information Center
   Ft. Belvoir, Virginia

2. Dudley Knox Library
   Naval Postgraduate School
   Monterey, California

3. Professor James H. Luscombe
   Naval Postgraduate School
   Monterey, California

4. Professor Nancy M. Haegel
   Naval Postgraduate School
   Monterey, California

5. LT Brian Rauscher
   United States Naval Reserve
   Monterey, California